

Deep Learning Computer Vision Algorithm for Detecting Kidney Stone Composition

Kristian M Black¹ MD, MSCR, Hei Law², Ali Aldouhki¹ MBBS, MS,

Jia Deng² PhD, Khurshid R Ghani¹, MBChB, MS, FRCS(Urol)

¹Department of Urology, University of Michigan, Ann Arbor, MI, USA

²Department of Computer Science, Princeton University, Princeton, NJ, USA

Authors contact information:

¹Medical Sciences Unit I, University of Michigan Medical School, 1301 Catherine St, Room 4432, Ann Arbor, MI 48109

²Department of Computer Science, Princeton University 35 Olden Street, Princeton, NJ 08540-5233

³ Medical Sciences Unit I, University of Michigan Medical School, 1301 Catherine St, Room 4432, Ann Arbor, MI 48109

⁴ Department of Urology, Room 114W, NCRC Building 16, University of Michigan, 2800 Plymouth Road, Ann Arbor, MI 48109

Corresponding author:

Kristian M Black, MD/MSCR

Email: krismbla@med.umich.edu

Telephone: +1 318-505-3830

University of Michigan, Medical Sciences Unit I, 1301 Catherine St, Room 4432, Ann Arbor, MI 48109

Keywords:

Ureteroscopy, Laser lithotripsy, Holmium, Computer Vision, Artificial Intelligence, Deep Learning

Abstract: 247; **Word count:** 1547

This is the author manuscript accepted for publication and has undergone full peer review but has not been through the copyediting, typesetting, pagination and proofreading process, which may lead to differences between this version and the [Version of Record](#). Please cite this article as [doi: 10.1111/bju.15035](https://doi.org/10.1111/bju.15035)

This article is protected by copyright. All rights reserved

Disclosures: KRG is a consultant for Boston Scientific and Lumenis; KRG has a scientific investigator grant from Boston Scientific. No funding was received for this study.

Author Manuscript

1
2
3
4
5
6
7
8
9
10
11
12
13
14
15
16
17
18
19
20
21
22
23
24
25
26
27
28
29
30
31

DR. KRISTIAN BLACK (Orcid ID : 0000-0002-3936-3752)

DR. KHURSHID R GHANI (Orcid ID : 0000-0002-6089-0733)

Article type : Original Article

Article Category: Translational Science

Abstract

Objectives: To assess the recall of a deep learning (DL) method to automatically detect kidney stones composition from digital photographs of stones.

Materials and Methods: 63 human kidney stones of varied compositions were obtained from a stone laboratory including calcium oxalate monohydrate (COM), uric acid (UA), magnesium ammonium phosphate hexahydrate (MAPH/struvite), calcium hydrogen phosphate dihydrate (CHPD/brushite) and cystine stones. At least two images of the stones, both surface and inner core, were captured on a digital camera for all stones. A deep convolutional neural network (CNN), ResNet-101 [ResNet, Microsoft], was applied as a multi-class classification model, to each image. This model was assessed using leave-one-out cross validation with the primary outcome being network prediction recall.

Results: The composition prediction recall for each composition were as follows: UA 94% (n=17), COM 90% (n=21), MAPH/Struvite 86% (n=7), Cystine 75% (n=4), CHPD/Brushite 71% (n=14). The overall weighted recall of the convolutional neural network's composition analysis was 85% for the entire cohort. Specificity and precision for each stone type were as follows: UA [97.83, 94.12], COM [97.62, 95] struvite [91.84, 71.43] cystine [98.31, 75], and brushite [96.43, 75].

Conclusion: Deep convolutional networks can be used to identify kidney stone composition from digital photos with good recall. Future work is needed to see if deep learning can be used for detecting stone composition during digital endoscopy. This technology may enable integrated endoscopic and laser systems that automatically provide laser settings based on stone composition recognition with the goal to improve surgical efficiency.

32

33

34 **Introduction**

35 There is increasing interest on optimizing holmium laser settings and techniques like
36 Dusting¹, as ureteroscopy (URS) and laser lithotripsy has become the predominant surgical
37 treatment for urinary stones in North America². Currently, stones are fragmented by selecting
38 pulse energy and frequency to break stones into either fine powder (dusting) or medium-sized
39 fragments for extraction. Laser energy needed to ablate stones varies with stone composition and
40 size³. Right now, surgeons manually choose laser settings based on a visual recognition of the
41 stone type and its durability. However, if settings could be automatically calculated based on
42 recognition of stone composition, this could improve the efficiency of lithotripsy. Furthermore,
43 because stone samples are often extracted with baskets for composition analysis to guide
44 management, an endoscopic visualization system reliably determines stone composition would
45 have benefits in reducing operative time and surgical costs.

46 Computer vision together with deep learning may offer a solution to these unmet needs.
47 Current state-of-the-art approaches to the image classification task, a computer vision task where
48 the computers categorize images, use deep neural networks to extract patterns from an image and
49 make prediction based on the patterns, permitting automatic prediction of outcomes. To date,
50 several studies have demonstrated the value of DL for recognizing pathologic features in
51 diseases such as melanoma and diabetic retinopathy^{4,5}. With its emergence as a powerful tool for
52 image-based analysis, we studied the recall of using convolutional neural networks (CNNs) for
53 detecting the composition of five main categories of human kidney stones. Establishing this
54 framework during URS could lead to the automatic selection of laser lithotripsy settings based on
55 real-time stone composition analysis.

56 **Materials and Methods**

57 Human kidney stones of varied compositions were obtained from a stone laboratory in
58 2018 (Louis C. Herring and Company, Florida) including calcium oxalate monohydrate (COM),
59 uric acid (UA), magnesium ammonium phosphate hexahydrate (MAPH/struvite), calcium
60 hydrogen phosphate dihydrate (CHPD/brushite) and cystine stones. All stones included in this
61 study were preserved in dry conditions in glass vials. Mean stone size was 5.7 mm (± 3.5 ; range
62 2-18 mm). Dry stones were placed on a green non-reflective background and pictures were taken

63 with a DSLR camera fitted with macro lens (55mm). At least two images of the stones, both
64 surface and inner core, were captured on a digital camera for all stones. Using Photoshop
65 (Adobe, CA), the green non-reflective background was manually removed from each photo using
66 the mask function and saved as JPG files. This was followed by randomly generated computer
67 automated cross-sectional cropping (Figure 1). While a pre-trained segmentation model such as
68 UNet is powerful, it is more suitable for tasks which require pixel-wise predictions. Since we are
69 classifying the stone composition, we picked the models that performed well on image
70 classification. We applied a deep CNN, ResNet-101 [ResNet, Microsoft], as a multi-class
71 classification model, to classify each image crop⁶. The average of the classification scores of 30
72 random crops was used for final prediction. We sampled crops of different sizes from an image
73 and we resized all of them to size 96 x 96 before we fed them into the deep CNN. We whitened
74 each crop using the RGB mean and standard deviation. The deep CNN was trained with the
75 resized and whitened crops to predict stone composition. All stone images used in the training set
76 were different from those used in the testing set. Since we only had limited amount of data, we
77 used a ResNet-101 that was pretrained on the ImageNet classification dataset, a large-scale
78 image classification dataset, to avoid overfitting. We replaced the fully connected layers in
79 ResNet-101 with a fully connected layer of 128 channels with Batch Normalization and ReLU
80 followed by another fully connected layer of 128 channels, which are both randomly initialized,
81 and a softmax layer for predicting the stone composition. Hence, we used the cross-entropy loss
82 function. During training, we fixed the weights in the convolution layers and only updated the
83 weights in the fully connected layers. We used stochastic gradient descent (SGD) with a learning
84 rate of 0.001, a momentum of 0.9 and a weight decay of 0.0001 to optimize the loss function for
85 2000 iterations across all stone types. We then reduced the learning rate to 0.0001 for another
86 2000 iterations. Hyperparameters were not chosen based on cross validation results. We used a
87 batch size of 128. To account for our small image dataset, instead of dividing the images into test
88 and train set, we assessed recall of the network using leave-one-out cross validation method,
89 where we used all stones except one as the training set and tested the network on the remaining
90 one. This was repeated until all stones were tested producing recall averages for each stone type.
91 Because sample size varied between stone compositions, an overall weighted average was also
92 calculated.

93 **Results**

94 A total of 63 stones were used including 17 UA, 21 COM, 7 struvite, 4 cystine, and 14
95 brushite stones comprising a total of 127 images (figure 2). Stone recognition prediction recall
96 (sensitivity) varied by composition. UA stones had the highest recall at 94% followed by COM
97 stones with 90%. Struvite and cystine stones were classified with moderate recall, correctly
98 identified 86% and 75%, respectively. Lower predictive recall was seen for brushite stones
99 (71%). Overall weighted prediction recall was 85%. Specificity and precision for each stone type
100 are as follows: UA [97.83, 94.12], COM [97.62, 95] struvite [91.84, 71.43] cystine [98.31, 75]
101 brushite [96.43, 75] (table 1). ROC curve, precision-recall curve, and our confusion matrix can
102 be found in figure 3. The training loss per iteration plot for one of the cross-validation
103 experiments is provided as a supplementary figure.

104 In an attempt to understand the accuracy of stone composition from endoscopic video
105 images, we analyzed still images of 3 COM stones and 1 UA stone taken during a flexible URS
106 case, through our deep CNN. The preliminary results, demonstrating feasibility, were as follows:
107 recall for COM=0.67, precision for COM=0.71; recall for UA=1.0, precision for UA= 0.5.

108

109 Discussion

110 In this pilot study, we have shown that it is possible to predict kidney stone composition
111 from digital photos using computer-vision and DL. Commonly encountered stones such as UA
112 and COM, had higher accuracies than stones such as brushite and cystine. These stones have
113 distinct visual appearances and are often the easiest for humans to identify. The lower prediction
114 scores for other stone compositions may be a reflection of the visual heterogeneity of these
115 stones. Brushite specifically has been noted as a difficult stone composition to classify with
116 computer vision methods due to its high level of intraclass variability⁷. To our knowledge, this is
117 the first report of using CNNs to predict kidney stone composition though other methods such as
118 Raman spectroscopy and autofluorescence have been studied^{8,9}.

119 Only one prior study assessed image-based methods to determine kidney stone
120 composition⁷. Serrat et al computed hand-crafted features from each image (e.g. local binary
121 pattern and color histogram) and applied a traditional machine learning approach (random forest)
122 to classify the features. They found an overall composition prediction accuracy of 63%. In their
123 model, pH was also included as an additional feature to improve stone composition prediction.
124 Using CNNs, we were able to produce higher accuracies without incorporating any hand-crafted

125 features. The main advantage of DL is that the CNN autonomously learns to extract features
126 useful for classifying stone composition directly from the image, eliminating manual feature
127 extraction and user bias.

128 Our study has several limitations. We used only pure stones and additional studies are
129 needed to predict the composition of mixed stones. We studied only still images, whereas during
130 URS, imaging is video-based and includes body wall movement with blood/debris. Future
131 studies will include predicting stone composition based on images taken during URS. Data
132 reported in this study may serve as a benchmark for future comparisons of kidney stone
133 composition detection during URS.

134 Our work lays the foundation for video-based recognition. Using CNNs, this would be
135 feasible, as previously shown for recognizing and tracking surgical instruments in robotic
136 surgery videos¹⁰. Another area of study is to determine if computer-vision can accurately detect
137 stone size. Size information can provide feedback on when the optimal fragment size has been
138 achieved for extraction or dusting. Lastly, we only had a limited set of stone imaging data. We
139 hypothesize the recall of stone recognition will improve if the DL network is able to train on a
140 larger set of data.

141 In conclusion, we have shown that a DL computer-vision algorithm can be used to detect
142 the composition of commonly encountered kidney stones. In the future, digital endoscopic
143 platforms that leverage AI and DL techniques could provide a cheaper and faster alternative to
144 traditional stone analysis. Similar systems could be adapted to smartphones to allow office-based
145 stone analysis. The ability to intraoperatively determine stone composition could result in the
146 development of integrated endoscopic and laser systems that automatically provide laser settings
147 based on computer-vision stone characterization with the goal to improve laser lithotripsy
148 efficiency. One caveat that must be noted is the need for computer vision result verification and
149 interpretation by a licensed clinician. While AI systems such as this have the ability to identify
150 pathology, these technologies do not possess the capacity to consider clinical conditions that can
151 impact the pathologic state and therefore should aid, not replace expert opinion.

152 REFERENCES

153

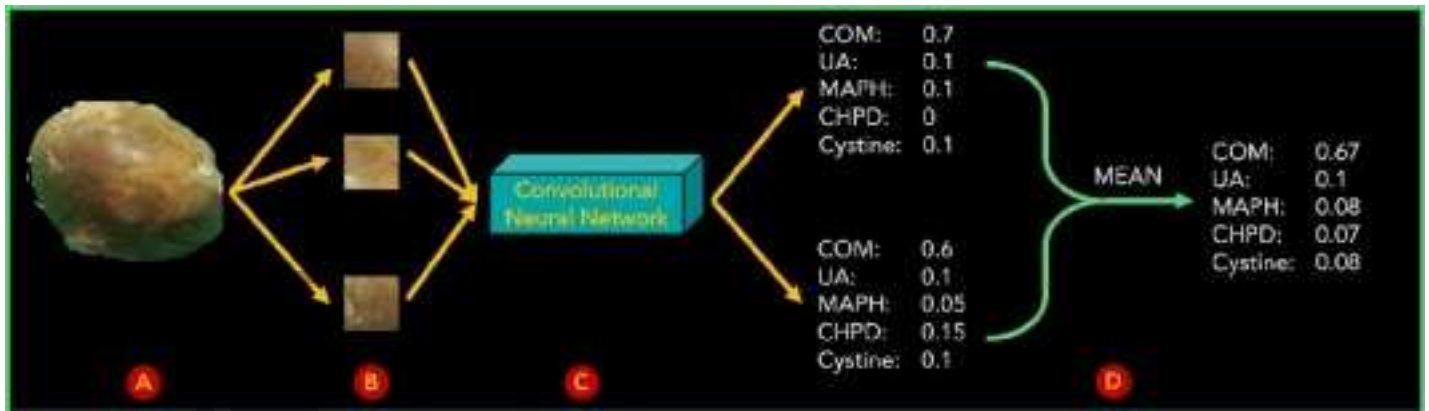
- 154 1. Dauw CA, Simeon L, Alruwaily AF, et al. Contemporary Practice Patterns of Flexible
155 Ureteroscopy for Treating Renal Stones: Results of a Worldwide Survey. *J Endourol.*
156 2015;29(11):1221-1230.
- 157 2. Ordon M, Urbach D, Mamdani M, Saskin R, RJ DAH, Pace KT. The surgical management
158 of kidney stone disease: a population based time series analysis. *J Urol.*
159 2014;192(5):1450-1456.
- 160 3. Vassar G.J. TJM, Glickman R.D. Holmium:YAG lithotripsy efficiency varies with energy
161 density. *J Urol.* 1998;160(2):471-476.
- 162 4. Esteva A, Kuprel B, Novoa RA, et al. Dermatologist-level classification of skin cancer with
163 deep neural networks. *Nature.* 2017;542(7639):115-118.
- 164 5. Gulshan V, Peng L, Coram M, et al. Development and Validation of a Deep Learning
165 Algorithm for Detection of Diabetic Retinopathy in Retinal Fundus Photographs. *JAMA.*
166 2016;316(22):2402-2410.
- 167 6. He K, Zhang X, Ren S, Sun J. Deep Residual Learning for Image Recognition. Paper
168 presented at: 2016 IEEE Conference on Computer Vision and Pattern Recognition
169 (CVPR); 27-30 June 2016, 2016.
- 170 7. Serrat J, Lumbreras F, Blanco F, Valiente M, López-Mesas M. myStone: A system for
171 automatic kidney stone classification. *Expert Systems with Applications.* 2017;89:41-51.
- 172 8. Schutz J, Miernik A, Brandenburg A, Schlager D. Experimental Evaluation of Human
173 Kidney Stone Spectra for Intraoperative Stone-Tissue-Instrument Analysis Using
174 Autofluorescence. *J Urol.* 2019;201(1):182-187.
- 175 9. Miernik A, Eilers Y, Bolwien C, et al. Automated analysis of urinary stone composition
176 using Raman spectroscopy: pilot study for the development of a compact portable
177 system for immediate postoperative ex vivo application. *J Urol.* 2013;190(5):1895-1900.
- 178 10. Law H, Ghani K, Deng J. Surgeon Technical Skill Assessment using Computer Vision based
179 Analysis. Proceedings of the 2nd Machine Learning for Healthcare Conference; 2017;
180 Proceedings of Machine Learning Research.

181

Table 1. Recognition performance measures by stone composition type for ResNet-101 CNN.

	Recall (Sensitivity)	Specificity	Precision (PPD)
	94.12	97.83	94.12
	90.48	97.62	95.00
	71.42	91.84	71.43
	75.00	98.31	75.00
	85.71	96.43	75.00

Author Ma



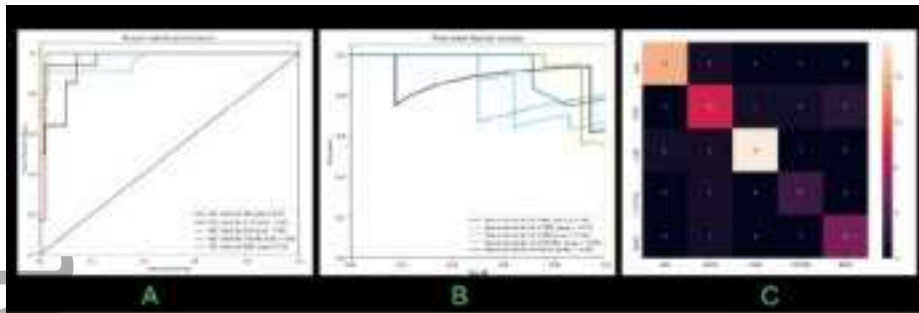
bj_u_15035_f1.png

Author Manuscript



bj_u_15035_f2.png

Author Manuscript



bj_u_15035_f3.png